XLIII CILAMCE
21–25, November, 2022
FOZ DO IGUAÇU – PR – BRAZIL

On the manufacturing condition estimation of spray nozzles via image processing and epicycle representation

Gabriel A. Costa[1], Fabrício C. L. Almeida[1], Marcos Silveira[1], Paulo J. P. Gonçalves[1]

[1]*Dept. of Mechanical Engineering, São Paulo State University - UNESP*
Av. Eng. Luiz Edmundo C. Coube 14-01, 17033-360, São Paulo, Brazil
gabriel.a.costa@unesp.br, fabricio.lobato@unesp.br, marcos.silveira@unesp.br, paulo.paupitz@unesp.br

Abstract. Defects on irrigation spray nozzles, occurred during the manufacturing process, can affect such distribution pattern leading to an uneven product application and increasing wastage. With a specific test bench, side-view images of hollow-cone nozzle sprays were collected as an attempt to assess the manufacturing condition of very brand-new nozzles. Classical image processing tools was applied on this side-view images, using a filter to reduce any spurious noise and the combined use of power-law transformation together with the contrast stretching technique to enhance image contrast, highlighting the presence of grooves in sprays, which is an indication of uneven distribution. An algorithm was develop to represent the spray as a contour with a few representative points, reduced from the large number of pixels and so compressing heavily the image size. These points were then used as input to estimate the spray format via epicycle representation carried out using a computation algorithm based on the discrete Fourier transform (DFT) leading to coefficients that are sensitive to the spray jet format. Samples of nozzles presenting no manufacturing defects was used to define threshold values for these coefficients, so that, any change in this regard can be an indication of manufacturing problems.

Keywords: hollow-cone nozzles, image processing, epicycle representation

1 Introduction

Spray nozzles are devices used to split liquid into a spray with specific pattern and distribution according to the desired application. Defects on nozzles change these characteristics, leading to a uneven distribution or waste of fluid, which in some cases may cause environmental damage (Ozkan et al. [1]; Zhang et al. [2]). Brand-new nozzles are generally tested on a specific bench used to verify any issue caused during the manufacturing procedures. This is carried out by trained human supervision, so that any undesired patterns in the spray that indicate defects can be visualized (detected), but such test can be subjective and dependent on the technician experience. For irrigation nozzles, however, studies concern the wear mechanism and how to predict its evaluation have been conducted on different basis of analysis, such as via experimental observation and numerical modelling up to some image processing approaches.

A controlled test bench was designed by Ozkan et al. [1], where a mixture of water and abrasive particles were used in an attempt to simulate the wear mechanism on nozzles, so that experimental analysis could be conducted to verify the spray pattern as a function of the wear level and the mixture flow rate. They observed that the spray width was not heavily affected, but the central region of spray presented a significant change. Replicating this experimental proceedings, Kecskésné Nagy et al. [3] analysed the spray quality based on the characteristics of droplets distribution and size by using a sensitive paper, so that the droplet scattering increment due to wear could be assessed. Another qualitative study was conducted by Siebald et al. [4] using acoustic sensors (accelerometers and microphone) to detect operational defects, studying the signal acquisition by attaching the sensors on the bench nozzle holder instead of attach on the nozzle, to allow a easy change of nozzles during the tests. Numerical simulations can also aid in understanding the wear mechanism in nozzles. Krishnaswamy and Krishnan [5] used a database of spray characteristics to develop a regression model, together with a neural network algorithm to predict nozzle wear evolution. Xu and Yan [6] developed a CFD based algorithm to analyse wear of nozzles by observing the fluid flow behavior, the mass loss rate of the orifice together with the effects on the pressure and velocity.

Image based studies analyse the visual effects of failures on the spray distribution pattern to identify the presence of defects. Cameras with high speed and resolution are largely used to collect high-definition images in order to visualise the spray's macro and micro characteristics. The combination of image processing techniques,

applying background subtraction, filtering and edge detection, associated with computational vision approach, were used to estimate the droplet size and spray distribution in some studies (Zhang et al. [2]; Sudheer and Panda [7]). Minov et al. [8] performed a comparison between digital images of distribution estimation with a patternator bench, which is essentially an array of parallel tubes collect the spray droplets at different distances leading to the spray distribution estimation. This image method seems to be promising as a non-intrusive technique. Çetin et al. [9] used intensity vectors collected from digital images, which in turn is a slice of the image (line of pixels) that contains some representative behavior of the nozzle's cross-section area, but reducing the size of the data analysed and can be used to estimate the spray distribution pattern.

The epicycle concept is widely developed and used in astronomy to define relative trajectory of astronomic bodies. The epicycle representation is also applied as an effective way to represent complex contour or trajectory as a sum of connected circles, being applied on position description or image reconstruction. Baiamonte and Baiamonte [10] used the concept of epicycle drawing to describe the distribution area pattern of a centre-pivot sprinkler nozzle, considering his orbital trajectory. Liang et al. [11] applied epicycle formulation to simulate complex shape particles, and using the estimated parameters to analyse the behavior of the interaction of these complex particles on the characteristics of granular materials.

The objective of this work is to investigate experimentally side-view images of sprays generated by hollow cone nozzles taken by an ordinary camera, as an attempt to estimate its manufacturing condition. Image processing techniques were used to enhance the spray images, and a method to represent the sprays as a few number of points representative of the spray profile (contour) was developed. An epicycle representation was applied to reach a numerical parameter to estimate the nozzle manufacturing condition.

2 Data acquisition and pre treatment

A test bench, provided by the company *Spraying Systems Co.*, was used to carry out experimental tests, so that visual assessment of the spray of nozzles could then be conducted. This bench allows strict control of the water pressure, which was set at 40 psi based on standards for nozzle tests (ISO 5682-1:2017). Figure 1(a) shows a broad view of the test bench and the GoPro camera used to record the spray jet image. Figure 1(b) shows a example of spray image for a nozzle in good condition, and Fig. 1(c) shows a schematic drawing of the bench and the camera used to carry out the tests.

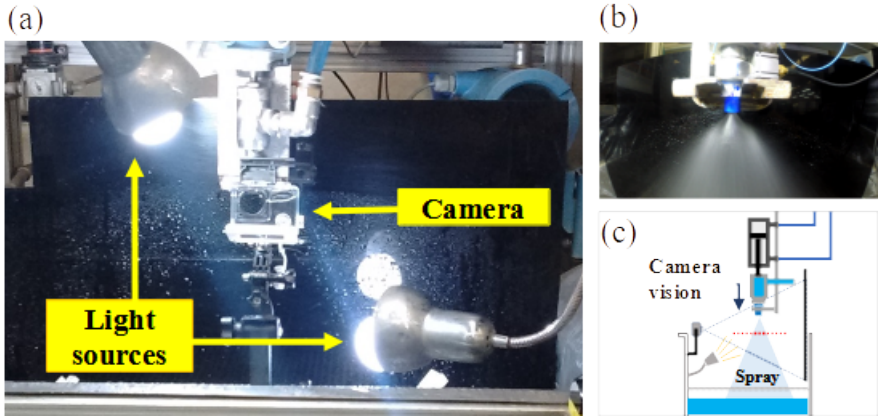

Figure 1. Description of test rig bench: (a) instrumentation and general view, (b) Example of spray photo collected, and (c) Schematic of the test bench and camera position

The GoPro camera was fixed on the test bench, so that the images were taken from still frames of a video recorded for 10 seconds at a frame rate of 60 fps and resolution of 1920x1080 pixels. Three nozzles previously tested by human supervision were used to investigate the feasibility of the technique herein investigated. The nozzles were labelled as N1 for a good condition nozzle, N2 for a moderate defective nozzle and N3 for a unacceptable working condition nozzle. Hence, the front view images of the spray jet were taken from each nozzle, aiming to visualize the presence of grooves which in turn are responsible for an uneven distribution when defects are present in such nozzles. The images was then converted to grayscale to reduce the data size, from a $m_x n_x 3$ RGB to a $m_x n$ intensity matrix, and improve computational efficiency for the processing.

2.1 Image Pre-processing procedures

The raw images taken during the tests presented some light spots due to droplets on the background, representing noises on the image data. A 2D Butterworth low-pass filter was applied to these images beforehand, to reduce the light spots. Moreover, a power-law transformation combined with a contrast stretching, which are two techniques used to enhance the contrast, were applied to highlight the intensity variations on the images.

The filtering procedure was conducted by using the image spectrum on spatial frequency domain via the 2D Fast Fourier Transform, following the representation given by Gonzalez et al. [12] with frequency units in $cycle/pixel$. In this domain, the the image spectrum was then multiplied by the Frequency Response Function (FRF) of the filter, and the inverse transform was applied afterwards to obtain a filtered image. Equation (1) shows the filter function, where u and v are the spatial frequencies, $D(u,v)$ defines the euclidean distance from the center of the spectrum ($D(u,v) = \sqrt{u^2+v^2}$), D_0 is related to the half-power frequency (frequency value in which the function has a $3dB$ reduction in amplitude) and o_d is the filter order.

$$H_b(u,v) = \frac{1}{1+[D(u,v)/D_0]^{2o_d}}. \tag{1}$$

The half-power frequency was set to $30cycle/pixel$, which is the value that reduces the intensity due to the presence of spikes in the data but keeps the characteristics of the spray condition, and the order was set to 8.

As mentioned previously, two classical image processing techniques were used to enhance the contrast, highlighting the intensity variations due to grooves caused by the presence of defects. The power-law transformation technique is conducted by setting the intensity level $i_f(p)$ of each pixel by a power factor γ (Gonzalez et al. [12]). For $\gamma < 1$ the output intensity are lesser than the input, and the image becomes darker. On the other hand if $\gamma > 1$ the output are higher than the input, and the image becomes brighter. The second technique is a contrast stretching method applied to enhance the image sensitivity by clipping the input intensity level at a selected lower (L_{in}) and higher (H_{in}) intensity bounds. The intensity level between these bounds is re-scaled to the interval from 0 (dark) to 1 (bright) afterwards. The resulting power-law-stretching technique was used to enhance the presence of grooves, making them brighter than any other feature present in the data, which is given by

$$i_s(p) = \begin{cases} 0, & \text{if } i_f(p) < L_{in} \\ \left[\dfrac{i_f(p)-L_{in}}{H_{in}-L_{in}}\right]^{\gamma}, & \text{if } L_{in} < i_f(p) < H_{in} \\ 1, & \text{if } i_f(p) > H_{in} \end{cases}. \tag{2}$$

The value of $\gamma = 2$ seemed to be a reasonable choice to enhance the effect of spray grooves. Besides, the stretching bound limits were set at $H_{in} = 0.25$ and $L_{in} = 0.75$, which turns the lower intensity values much darker without affecting the brightness of the grooves. The first was selected based on the maximum level where noise due to water drops can be found, and the other one was related to the highest intensity level where grooves are likely found. Figure 2 shows a comparison between raw and pre processed images, filtering and contrast enhancement, for the three nozzles used for this investigation.

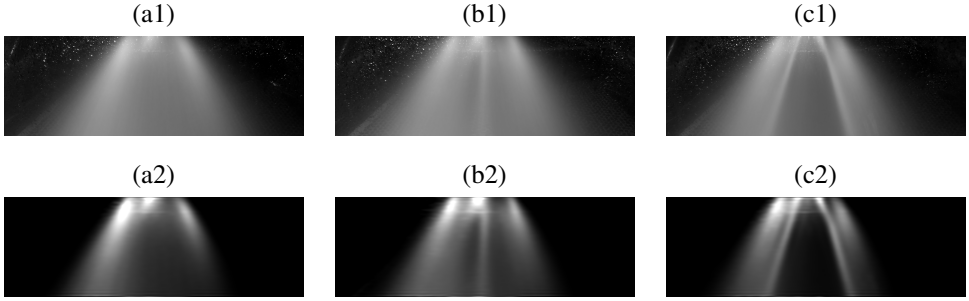

Figure 2. Comparison between (i) raw and (ii) pre-processed images for the nozzles (a)N1, (b)N2 and (c)N3

It is observed that the pre-processing procedure highlights the main visual characteristics of the images as depicted in Fig. 2, specially the defects on distribution pattern for the N2 and N3 nozzles. The pre-processed images are used as the input for the development of the following method to indicate the nozzle health condition.

3 Results

The method described as following was developed and investigated as an alternative way to assess the health condition of hollow cone nozzles and, perhaps, can be used as an autonomous technique to aid in estimating the nozzle health condition. Hence, an algorithm was designed to represent the spray profile by selecting a set of points representative of its distribution and groove patterns leading to a spray profile estimation that can be reconstructed via using epicycle reconstruction concept. This new method is described in the following section.

3.1 Spray profile representation using a set of points

Aiming a data size reduction, and considering the pattern behavior along the spray, 5 horizontal lines on spray images were selected as one way of representing intensity vectors. These lines are highlighted in Fig. 3 (ai), (bi) and (ci) for the nozzles N1, N2 and N3, respectively. An specific algorithm was developed, based on derivative maximum point, to find the maximum peaks in the intensity vectors given by along each line considering a threshold value where the slope gradient can rely within to avoid small fluctuations present in these lines. It is expected that the profile generated by the set of points for nozzles present good condition will depic only two peaks regarding the highest intensity levels located at the spray image edges (contour profile). However, for the defective ones it is expected more than two peaks due to the presence of grooves on the spray images, indicating a possible manufacturing problem. Figures 3(aii), (bii) and (cii) show the intensity vector of the first (top blue line) and last (botton red line) lines given in Fig. 3(i) as a function of the normalized pixel to the highest horizontal pixel (normalized pixel x) of the image for the N1, N2 and N3 nozzles, respectively. It is also depicted the set of points (black dot points) estimated using the methodology described previously.

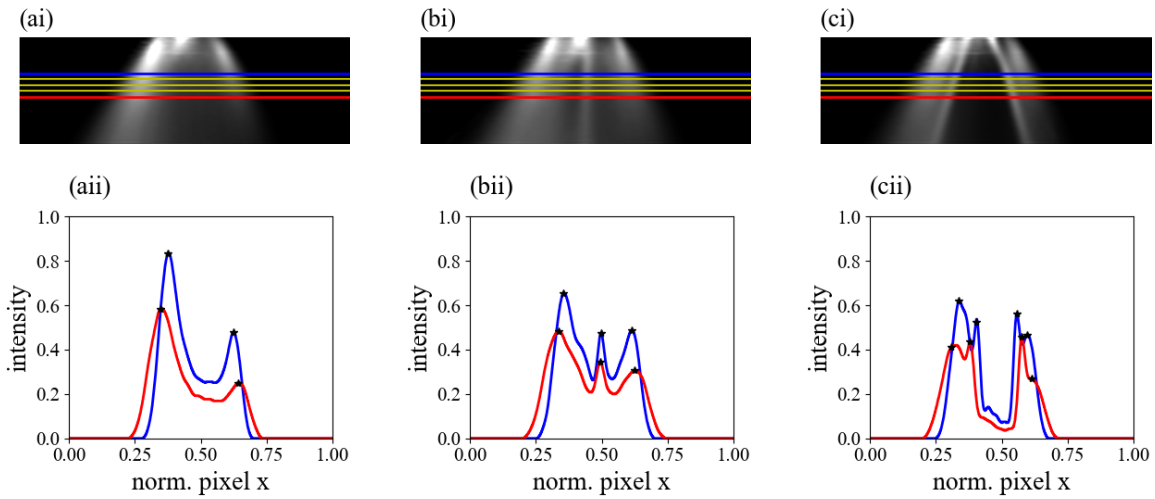

Figure 3. Lines selected on the images to represent intensity vectors for nozzles (ai) N1, (bi) N2 and (ci) N3; First and last intensity lines and correspond intensity peak points, for (aii) N1, (bii) N2 and (cii) N3

Once found the peaks for all the 5 lines from each image, the spray profile can be then estimated (reconstructed). Figure 4(a), (b) and (c) show these representative points of the spray profile for the N1, N2 and N3 nozzles. Furthermore, the position of each intensity line was normalized for convenience.

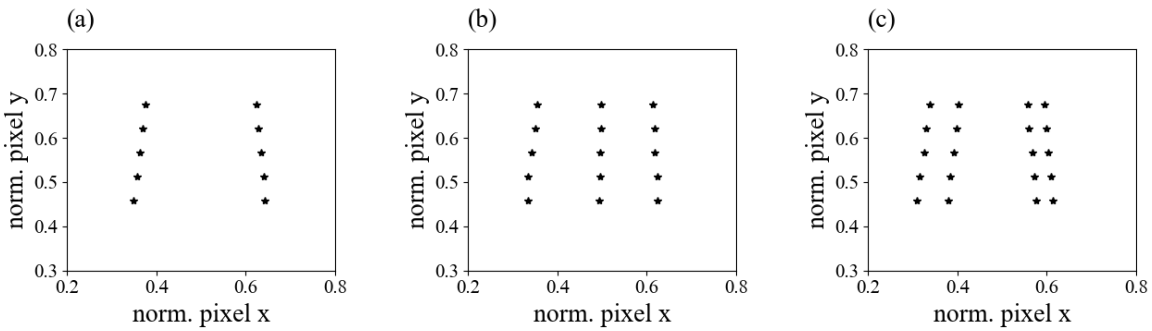

Figure 4. Spray profile as intensity lines peaks on a image position plane, for (a) N1, (b) N2 and (c) N3

3.2 Profile estimation using epicycle reconstruction

The epicycle reconstruction of any image, such as the spray profile, uses a Fourier based representation to compose an amount of circles connected to each other and rotating at frequencies multiple of the fundamental one, which are responsible for drawing an estimation such profile. Considering the profile on a complex plane coordinate, so that its is possible to have a function, $f_c(x)$, which can represent the shape with a cycle of 2π. The epicycles can be evaluated as a complex Fourier series, where the coefficients c_n are used to express the function as weighted sum of harmonic functions at different frequencies, amplitude and phases (from c_n being a complex number), these last two associated with the circles as radius and initial positions for each circle that composes the epicycles. Hence, the epicycle representation of the trajectory function can be obtained by the eq. (3), where i is the imaginary number.

$$f_c(x) = \sum_{n=0}^{\infty} c_n \, \mathrm{e}^{nix}, \tag{3}$$
$$c_n = \frac{1}{2\pi} \int_0^{2\pi} f_c(x) \, \mathrm{e}^{-nix} \, dx.$$

The epicycles components c_n are calculated using the FFT considering a finite number of N terms, where $n = 0, 1, ..., (N-1)$. To compose the spray profile reconstruction, the first circle is set at the center of the reference system (origin of the coordinates) and the radius and phase (c_0) leads to the centroid of the profile, which in turn gives the DC component. The second circle is built on the top of the first one starting from the point where c_0 is defined and so on. Overall, each circle is a rotating vector, apart from the one which c_0 is defined. This procedure repeats in sequence for the subsequent circles, so that the profile reconstruction is conducted using the position of the rotating vector given by the components of the latest circle. Then, the circles rotate along a period multiples of 2π, being each circle with a specific frequency, reconstructing the estimated profile.

The developed epicycle computation algorithm was applied to the spray profiles given by Fig. 4(a), (b) and (c). The number of points for the spray profile were increased by adding extra points within the existent ones via simple straight line interpolation. This procedure was carried out to give a smoother profile estimation using $N = 60$ components. Figure 5(a), (b) and (c) show the spray profile together with the reconstructed profiled (red solid line) performed via the epicycles for the N1, N2 and N3 nozzles, respectively.

It is observed that the profile reconstruction via the epicycles overlay very well the actual points obtained during the pre-processing procedures. It is also observed that the epicycle for the N2 case(Fig. 5(b)) presented a deviation from the actual data due to the way in which the developed algorithm reconstructs the profile. This, however, can be beneficial to the proposed fault detection method when using this technique as it can generated a very different profile from the one expected for a healthy nozzle (Fig. 5(a)). Figure 6(a), (b) and (c) show the modulus of the c_n terms as a function of each frequency for the N1, N2 and N3 cases, respectively. This term is related to the radius of each epicycle and will be used in the amplitude label for convenience. The DC component does not add any additional information with respect to the health nozzle condition. It just shows where the epicycle representation starts, so it will be neglected for convenience.

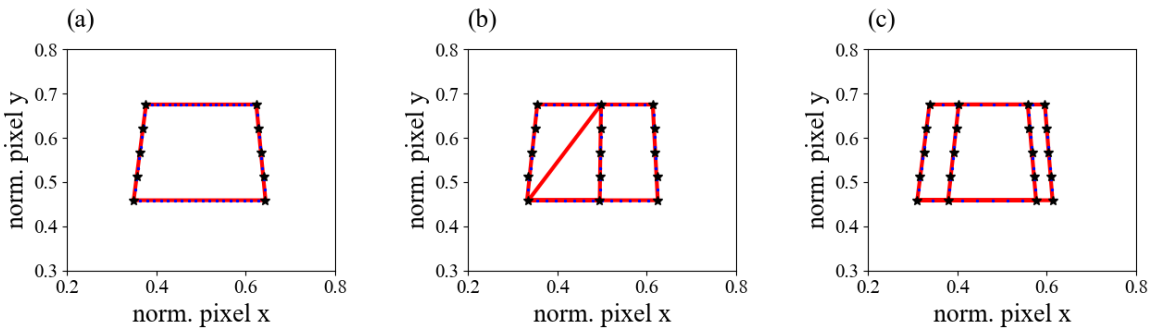

Figure 5. Epicycle reconstruction of each spray profile, for (a) N1, (b) N2 and (c) N3

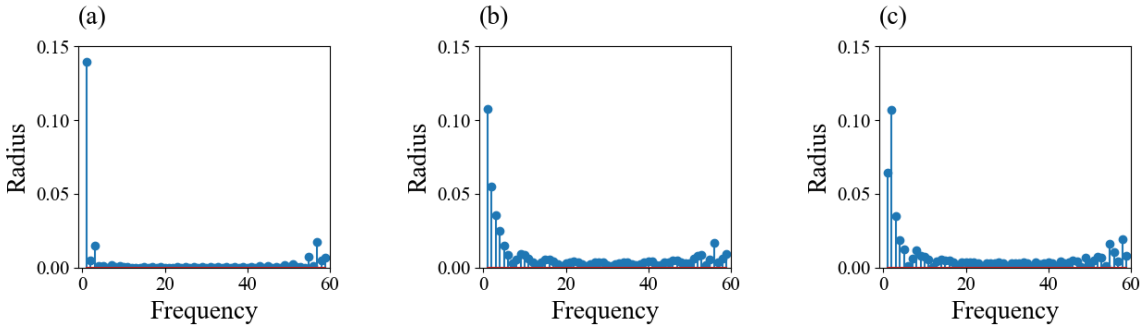

Figure 6. Epicycle parameters frequency vs radius, for (a) N1, (b) N2 and (c) N3

It is observed that for the good nozzle the highest epicycle radius is given by the $n = 1$ (c_1) term. Although it is possible to see some high frequency content due to the corners of the profile, the c_1 term dominates the frequency content depicting he good nozzle characteristic. This is not the case for the other two defective nozzles (N2 and N3). The first presents a frequency content spread mainly within the 5 components. The latter shows similar trend, but the third component shows the highest radius. These characteristics can be used to define when a nozzle presents a defected caused during its manufacturing.

4 Conclusions

The methodology herein described is carried out to detect defective nozzles due to manufacturing issues. Moreover, it is based on photos of the nozzle spray taken via using an ordinary camera and a especial bench. This methodology is performed in two steps. The first is a pre-processing procedure to enhance the main patterns that can be used to indicate a manufacturing defect, such as grooves. This step involves image filtering to reduce undesirable noise due to water drops in the background together with contrast enhancement procedures to make grooves brighter than any other feature in the image. The spray profile with (defective nozzles) and without (healthy nozzles) grooves can be estimated via selected few representative points, which are used to reconstruct the shape/contour using epicycle concepts. It was shown that the epicycle radius for the healthy nozzle is dominated mainly by the first component, which is not the case for the defectives ones. The epicycle radius are dominant for up to the fifth component highlighting the presence of grooves in the data. Although high frequency components appear in any reconstructed profile, related to the corner of the profile produced by the representative points.

Acknowledgements. The author would like to acknowledge CAPES (Grant # 88882.432844/2019-01) for the financial support given to this project and to Spraying Systems Co. to support the experimental tests.

Authorship statement. The authors hereby confirm that they are the sole liable persons responsible for the authorship of this work, and that all material that has been herein included as part of the present paper is either the property (and authorship) of the authors, or has the permission of the owners to be included here.

References

[1] H. E. Ozkan, D. L. Reichard, and K. D. Ackerman. Effect of orifice wear on spray patterns from fan nozzles. *Transactions of the ASAE*, vol. 35, n. 4, pp. 1091–1096, 1992.
[2] N. Zhang, L. Wang, and G. E. Thierstein. Measuring nozzle spray uniformity using image analysis. *Transactions of the American Society of Agricultural Engineers*, vol. 37, n. 2, pp. 381–387, 1994.
[3] E. Kecskésné Nagy, M. Koszel, and I. Sztacho-Pekary. Effect of working parameters and nozzle wear rate onto the spray quality in use of different fan flat nozzle. *Journal of Central European Agriculture*, vol. 15, n. 1, pp. 0–0, 2014.
[4] H. Siebald, O. Hensel, H.-H. Kaufmann, and S. Kirchner. Spray nozzle function control using acoustics for agricultural applications. *Biosystems Engineering*, vol. 197, pp. 149–155, 2020.
[5] M. Krishnaswamy and P. Krishnan. Pm - power and machinery: Nozzle wear rate prediction using regression and neural network. *Biosystems Engineering*, vol. 82, n. 1, pp. 53 – 64, 2002.
[6] Y. Xu and H. Yan. Numerical simulation of erosive wear on an impact sprinkler nozzle using a remeshing algorithm. *International Journal of Fluid Machinery and Systems*, vol. 9, n. 4, pp. 287–299, 2016.
[7] K. P. Sudheer and R. K. Panda. Digital image processing for determining drop sizes from irrigation spray nozzles. *Agricultural Water Management*, vol. 45, n. 2, pp. 159–167, 2000.
[8] S. Minov, F. Cointault, J. Vangeyte, J. Pieters, and D. Nuyttens. Spray nozzle characterization using a backlighted high speed imaging technique. *Aspects of Applied Biology*, vol. 122, pp. 353–361, 2014.
[9] N. Çetin, C. Sağlam, and D. B. Determination of spray angle and flow uniformity of spray nozzles with image processing operations. *The Journal of Animal and Plant Sciences*, vol. 29, n. 6, pp. 1603–1615, 2019.
[10] G. Baiamonte and G. Baiamonte. Using rotating sprinkler guns in centre-pivot irrigation systems. *Irrigation and Drainage*, vol. 68, pp. 893–908, 2019.
[11] Z. Liang, X. Wang, J. Gong, and Z. Nie. Random generation of 2d geometry-controlled particles via the epicycle series. *Granular Matter*, vol. 22, n. 84, 2020.
[12] R. C. Gonzalez, R. E. Woods, and S. L. Eddins. *Digital Image Processing*. Pearson Pretice Hall, New Jersey, 3 edition, 2008.